Carbohydrate Polymers 176 (2017) 356–364

Contents lists available at ScienceDirect

Carbohydrate Polymers

journal homepage: www.elsevier.com/locate/carbpol

Geraniol grafted chitosan oligosaccharide as a potential antibacterial agent

Lin Yue*, Jingru Li, Wanwen Chen, Xiaoli Liu, Qixing Jiang, Wenshui Xia*

State Key Laboratory of Food Science and Technology, School of Food Science and Technology, Collaborative Innovation Center of Food Safety and Quality Control in Jiangsu Province, of Jiangnan University, Lihu Road 1800, Wuxi, 214122 Jiangsu, People's Republic of China

ARTICLE INFO

Article history:
Received 24 January 2017
Received in revised form 10 July 2017
Accepted 14 July 2017
Available online 19 July 2017

Keywords:
Chitosan oligosaccharide
Geraniol
Solubility
Antibacterial activity

ABSTRACT

The novel derivatives of geraniol grafted chitosan oligosaccharide were synthesized via substitution and deprotection reaction, respectively. The products were identified by Fourier transform infrared (FT-IR), ^{1}H nuclear magnetic resonance (NMR), X-ray diffraction analysis (XRD), Thermogravimetric analysis (TGA) and UV–vis absorption spectroscopy. It is revealed that the derivatives exhibited a good solubility, thermal stability and antibacterial properties.

1. Introduction

Geraniol (Ger), a natural component of plant essential oils, having a roselike odor and taste, is generally used as a fragrance/flavor in the food industry to treat infectious diseases and/or preserve food (Burt, 2004; Cassani, Tomadoni, Viacava, Ponce, & Moreira, 2016; Solorzano-Santos & Miranda-Novales, 2012; Tomadoni, Cassani, Moreira, & Ponce, 2015). It is claimed to have various interesting applications including insect repellent, antimicrobial, antioxidant, anti-inflammatory and anticancer (Chen & Viljoen, 2010; Yegin, Perez-Lewis, Zhang, Akbulut, & Taylor, 2016).

Chitosan oligosaccharide (COS) is the hydrolyzed product of chitin and chitosan with solubility in neutral aqueous solutions due to its shorter chain lengths and free amino groups in D-glucosamine units (Jayakumar et al., 2010; Jeon & Kim, 2000), therefore COS has a smaller molecular size and lower viscosity than chitosan. There are two types of reactive functional groups, two hydroxyls at the 3, 6-carbon position and an amino group at the 2-carbon position which can be readily subjected to chemical derivatization. COS exhibits numerous biological functions such as antifungal, antibacterial, antitumor, anti-inflammatory and antioxidant activities (Choi et al., 2001; Huang, Mendis, Rajapakse, & Kim, 2006; Jeon & Kim, 2000; Rahman, Hjeljord, Aam, Sørlie, & Tronsmo, 2014; Shen, Chen, Chan, Jeng, & Wang, 2009; Sun, Yao, Zhou, & Mao, 2008; Xia, Liu, Zhang, & Chen, 2011; Zou et al., 2016). These biological activities are dependent on their physicochemical properties, which allow COS to be considered as a potential novel food ingredient (Vela Gurovic et al., 2015). Meanwhile, COS exerts antimicrobial effects against different groups of microorganisms. Therefore, it has also been used as an antibacterial agent and additive to improve the shelf life of food products (Kim & Rajapakse, 2005). The antibacterial activity of COS is low, whose chemical modification may lead to enhancement of its antibacterial activity. Previously, COS (CS) was modified with Kojic Acid (Liu, Xia, Jiang, Xu, & Yu, 2014), fumaric acid (Feng & Xia, 2011), and monomethyl fumaric acid (MFA) (Khan, Ullah, & Oh, 2016; Wang et al., 2015). Fumaric acid, Kojic Acid, and MFA are good antibacterial agents; they have shown no toxicity and can be used as a food preservative. The antibacterial activity of these COS (CS) derivatives has been effectively improved.

Our group had previously developed an antibacterial agent through kojic acid grafted COS. Both COS and kojic acid are good natural food preservatives; the safety of the derivative synthesized by them is guaranteed as a potential antibacterial agent (Liu, Xia et al., 2014). Based on our previous work, we have focused on essential oils, which have rich natural antibacterial constituents (Bakkali, Averbeck, Averbeck, & Idaomar, 2008; Burt, 2004; Kalemba & Kunicka, 2003). Essential oils are particularly enticing for antibacterial agents because they not only can inhibit several pathogens but also are nontoxic and natural antibacterial agents. Ger is a natural component of essential oils possessing antibacterial prop-

* Corresponding author.
E-mail addresses: yuelin@jiangnan.edu.cn (L. Yue), xiaws@jiangnan.edu.cn (W. Xia).

http://dx.doi.org/10.1016/j.carbpol.2017.07.043
0144-8617/

erty. Although Badawy and his co-workers reported application of Ger to improve chitosan products' antimicrobial activity, they simply added Ger into chitosan solution and tested this material as a film for food packing industry (Badawy, Rabea, Taktak, & El-Nouby, 2016). No existing research is involved regarding Ger grafted COS or other polymers and its antibacterial activity. Our study presents a concise preparation of chitosan oligosaccharide derivatives (COS-O-Ger) through substitution of hydroxyl group on COS with Geranyl Bromide. The chemical structure of COS-O-Ger was characterized by FT-IR, ^{1}H NMR, TGA, XRD and UV–vis. The antibacterial activity of COS-O-Ger against *Staphylococcus aureus* and *Escherichia coli* was also studied. Because COS and Ger are both good natural food preservatives, the preparation of COS-O-Ger could be interesting for some applications because it may combine the advantages of the two compounds and is expected to supplement each other for their antimicrobial activity. This investigation demonstrates the novel derivation of COS with geraniol that provides for a new antimicrobial agent against gram negative and gram positive bacteria. The safety of the new antimicrobial agent will be considered in a follow-on publication.

2. Materials and methods

2.1. Materials

The COS (Mw = 1 k Da) was made from crab shell and provided by Zhejiang Jinke Biochemical Co. Ltd. (Zhejiang, China) with the deacetylation (DA) of 90%. Ger ((*E*)-3, 7-dimethyl-2, 6-octadien-1-ol) was purchased from Shanghai Aladdin Biochemical Technology Co. Ltd. (Shanghai, China). Other chemical reagents were purchased from Sinopharm Group Chemical Reagent Co., Ltd. (Shanghai, China); all of them were of analytical grade and used directly with no further purification. *Staphylococcus aureus (ATCC120627)* and *Escherichia coli (ATCC25992)* used for the antibacterial assay were obtained from the School of Food Science and Technology of Jiangnan University. All water used in the extraction and analysis was distilled and deionized.

2.2. Synthesis of COS-O-Ger

COS-O-Ger was synthesized as follows (Fig. 1). An efficient procedure to prepare COS-O-Ger was established by using a three-step reaction. The NH_2 groups on COS were protected by benzaldehyde. Geranyl Bromide was prepared by Ger and phosphorus tribromide. The *N*-benzylidene COS was selectively grafted with Geranyl Bromide in *N*, *N*-Dimethylformamide (DMF), and then the COS-O-Ger was obtained by removing the benzylidene group of the protected COS. The ultimate yield of COS-O-Ger was 40.7%.The synthesis scheme of COS-O-Ger was as follows:

2.2.1. Synthesis of N-benzylidene COS

The *N*-benzylidene COS was synthesized according to a previous Schiff base method (Guo et al., 2007) with some modifications in order to protect the NH_2 groups of COS. Briefly, COS (0.025 mol) was dissolved in a solution of 1% acetic acid (70 mL) and diluted with methanol (100 mL), and then 110 mL of benzaldehyde/methanol 1:10 (v/v) was added dropwise into the COS solution over 30 min. The mixture was stirred at 60 °C for 3 h to obtain *N*-benzylidene COS. After the reaction was completed, the pH of the reaction mixture was adjusted to be 13.0 using 1 M NaOH. The residue was separated with a centrifuge and extracted in a Soxhlet apparatus with anhydrous ethanol to remove the extra benzaldehyde, subsequently dried in vacuum at 45 °C for 24 h (75.6% yield).

2.2.2. Synthesis of geranyl bromide

Geranyl Bromide ((2*E*)-1-Bromo-3, 7-dimethylocta-2, 6-diene) was synthesized by referencing the relevant literature (Murphy & Taggart, 2001). Ger (0.025 mol) and phosphorus tribromide (0.01 mol) were stirred in anhydrous diethyl ether at −5 °C for 30 min. After the reaction completed, the solution was poured into the separatory funnel to extract organic phases with sodium bicarbonate solution (5%) and saturated salt water in turn, and then it was dried with anhydrous magnesium sulfate and filtered. Finally, the products were obtained by vacuum distillation (99.9% yield). The Geranyl Bromide was applied directly to the next step response without purification.

2.2.3. Synthesis of COS-O-Ger

We prepared COS-O-Ger with different degree of substitution (DS), named COS-O-Ger1, COS-O-Ger2 and COS-O-Ger3, respectively. Specifically as follows:

Firstly, different molar ratios of Geranyl Bromide and *N*-benzylidene COS (1:1, 2:1 and 3:1) were separately dissolved in DMF, and then *N*-benzylidene COS solution was added dropwise to Geranyl Bromide solution, and then pyridine was added as a catalyst. The reaction mixtures were stirred at room temperatures for 6 h to obtain COS-O-Ger solution (Liu, Xia et al., 2014). The resulting solution was precipitated and washed repeatedly with acetone, then extracted in a Soxhlet apparatus with petroleum ether for 24 h, finally dried in vacuum at 45 °C for 12 h to obtain *N*-benzylidene COS-O-Ger. *N*-benzylidene COS-O-Ger was dissolved in a mixture containing ethanol and 0.25 mol/L hydrochloric acid solution (4:1 v/v) at room temperature for 24 h to deprotection (Yan et al., 2016). The resulting solution was allowed to precipitate by adjusting pH to neutral with Na_2CO_3. The precipitate was collected by filtration and extracted in a Soxhlet apparatus with anhydrous ethanol for 24 h, subsequently dried in vacuum at 45 °C for 12 h to obtain the product (53.9% yield).

2.3. Characterization and measurements

2.3.1. Elemental analysis

Elemental analysis was performed by using an element analysis instrument (Vario EL III, Elementar Analysensysteme GmbH, Germany). The particulate organic carbon and nitrogen mass percentages of four samples of COS and derivatives were obtained. The DS of COS-O-Ger1-3 were calculated based on carbon–nitrogen ratio (Dos Santos, Caroni, Pereira, da Silva, & Fonseca, 2009). The DS was calculated by a previously described method (Wang & Wang, 2011) in Supporting Information (Supplemental Formulae 1).

2.3.2. UV–vis spectroscopy

UV–vis absorption spectra of pure Ger, blank COS and COS-O-Ger solutions 0.2% (w/v) were recorded using a UV 1000 spectrophotometer (Techcomp Ltd., China). Deionized water was the blank solution in the spectral region of 190–800 nm with a beam width of 2 nm.

2.3.3. FT-IR spectroscopy

The presence of functional groups of the pure Ger, blank COS and COS-O-Ger was analyzed using a Nicolet Nexu S470 instrument (Nicolet Instrument, Thermo Co., Madison, WI, USA). All the samples were prepared as KBr pellet and scanned against a blank KBr pellet background at a resolution of 4.0 cm^{-1} with the wave number range between 4000 and 400 cm^{-1}.

2.3.4. ^{1}H NMR spectroscopy

^{1}H NMR spectra were obtained on a 400 MHz NMR (Bruker, Germany) by operating at 25 °C. COS was dissolved in D_2O, with 4, 4-dimethyl-4-silapentane-1-sulfonic acid (DSS) as the internal

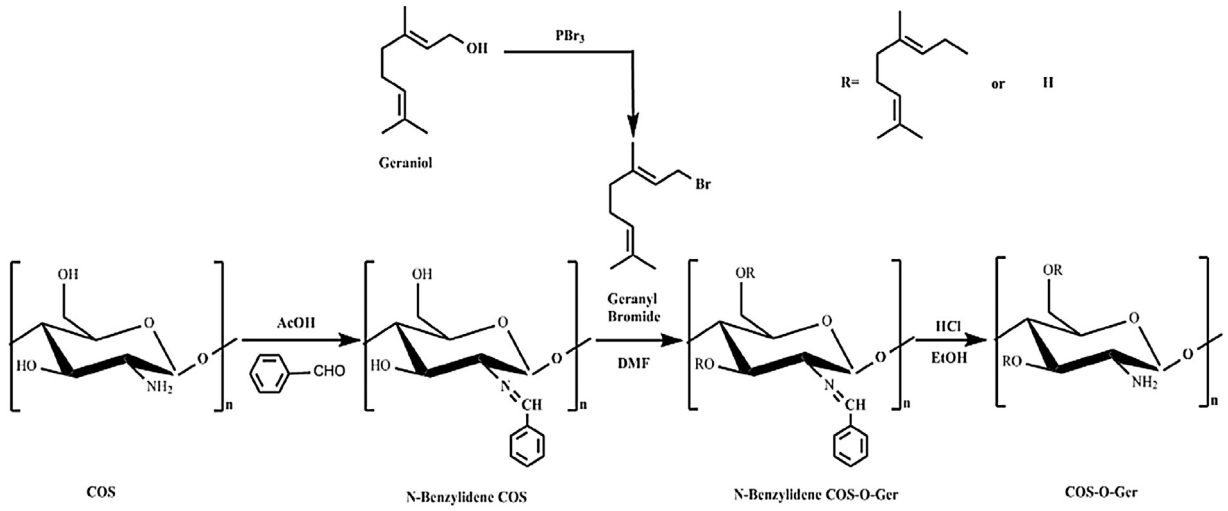

Fig. 1. Synthetic pathway for the preparation of COS-O-Ger.

standard. Ger and COS-O-Ger were dissolved in $(CD_3)_2SO$, with tetramethylsilane (TMS) as the internal standard.

2.3.5. X-ray diffraction (XRD)

X-ray diffraction (XRD) patterns of samples were recorded using an X-ray diffractometer (D8 Advance, Bruker, Germany). Advance diffractometer with an area detector was operating at a voltage of 40 kV and a current of 50 mA at Cu Kα radiation of k = 0.154 nm. The scanning rate was 2°/min, and the scanning scope was set from 5° to 80° at the room temperature.

2.3.6. Thermogravimetric analysis (TGA)

The decomposition pattern of the samples was made on a Mettler Toledo TGA2 thermogravimetric analyzer (Zurich, Switzerland) under the nitrogen atmosphere with a flow rate of 20 mL/min^{-1} to analyze the thermal stability of the samples. The sample (3 mg) was heated from 30 to 550 °C at a heating rate of 20 °C/min^{-1}.

2.4. Solubility test

Ger was dispersed in distilled water and different organic solvents (1:1 v/v) including anhydrous ethanol, acetone, diethyl ether, glacial acetic acid, DMSO and DMF at room temperature (25 °C), respectively. 25 mg COS or newly synthesized COS-O-Ger1-3 was respective dispersed in 5 mL distilled water (pH 7.0 ± 0.04) and above six different organic solvents (Ma, Yang, Kennedy, & Nie, 2009). The solutions were evaluated at room temperature (25 °C) with stirring for 1 h. The extent of solubility was represented as completely soluble, partially soluble or swell and insoluble. To evaluate the effect of pH on water solubility of COS-O-Ger1-3, sample was dissolved in HCl solution (0.1 M) to reach 5 mg/mL concentration. With stepwise addition of NaOH solution (0.1 M), the transmittance of the solution was recorded by using a UV 1000 spectrophotometer (Techcomp Ltd., China) at 600 nm (Feng & Xia, 2011).

2.5. Antibacterial activity

The antibacterial activities of COS, Ger and COS-O-Ger1-3 were tested using a modified colony counting method. A Gram-negative and Gram-positive organism (*E. coli and S. aureus*) were used as the test organisms. The strains were picked off with a wire loop, grown in nutrient broth (1% peptone, 0.3% beef extract, and 0.5% NaCl, pH 7.2 and sterilized at 121 °C for 20 min), and then incubated at 37 °C in an incubator shaker over night prior to the testing (Liu, Xu et al., 2014). From this primary culture secondary cultures were obtained in 100 mL nutrient broth in conical flasks, and the bacterial suspension was adjusted to the turbidity of MacFarland standard 0.5 (Másson et al., 2008) and further diluted with sterile normal saline solution (0.85%, w/v) to get concentration of about 5 ± 0.08 Log CFU/mL. Under aseptic condition the bacterial suspension (2.5 ± 0.1 μL) was inoculated into 5.00 ± 0.05 mL of nutrient broth containing 10.0 ± 0.1 mg of COS, Ger, and COS-O-Ger1-3, respectively, whereas a blank control was also prepared without test materials for comparison. Then all of the samples were incubated for 6 h at 120 rpm. 50.0 ± 0.1 μL of these cultures were spread on nutrient broth agar plates and incubated for 16 h (Ahmad, Ahmed, Swami, & Ikram, 2015).

3. Results and discussion

3.1. Characterization of COS-O-Ger

3.1.1. UV–vis spectroscopy analysis of COS-O-Ger

The UV–vis absorption spectra of COS and COS-O-Ger1-3 dilute aqueous solution and Ger dilute ethanol solution were shown in Fig. 2 to prove the existence of a chemical bond. Ger exhibited two characteristic absorption bands at 217 and 239 nm, which were probably caused by the C=C double bond and —OH group (Liu, Lu, Kan, Tang, & Jin, 2013) to intraligand $\pi \rightarrow \pi^*$ and $n \rightarrow \sigma^*$. In the UV–vis spectrum of COS, one absorption band (at 200 nm) and the other broad absorption band (at 305 nm) were observed, which might be probably ascribed to free amino groups (Aljawish et al., 2012) and the C=O group of COS, respectively, whereas these bands were assigned to intraligand $n \rightarrow \pi^*$ and $\pi \rightarrow \pi^*$ (Moreno-Vasquez et al., 2017). When Ger was grafted onto COS, two absorption bands of Ger at 217 and 239 nm shifted respectively to 200 and 249 nm, which were assigned to intraligand $n \rightarrow \pi^*$ and $\pi \rightarrow \pi^*$ transitions group. This indicated that COS-O-Ger1-3 were synthesized successfully.

3.1.2. FT-IR spectroscopy analysis of COS-O-Ger

The FT-IR spectra of COS and COS-O-Ger1-3 were shown in Fig. 3 and the FT-IR spectra of other intermediate products were provided in Supporting Information (Supplemental Figs. 1 and 2). In the FT-IR spectrum of COS, the broad band at around 3387 cm^{-1} was contributed by the stretching vibration of —NH_2 and —OH group (Liu, Liu, Yue, Jiang, & Xia, 2016), as well as inter- and intra-molecular

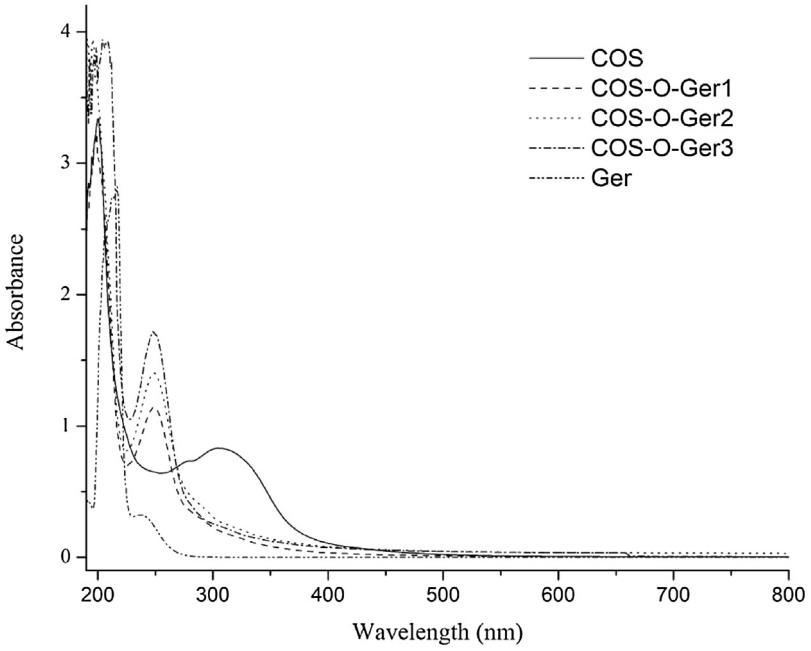

Fig. 2. UV–vis spectra of COS, Ger, and COS-O-Ger1-3.

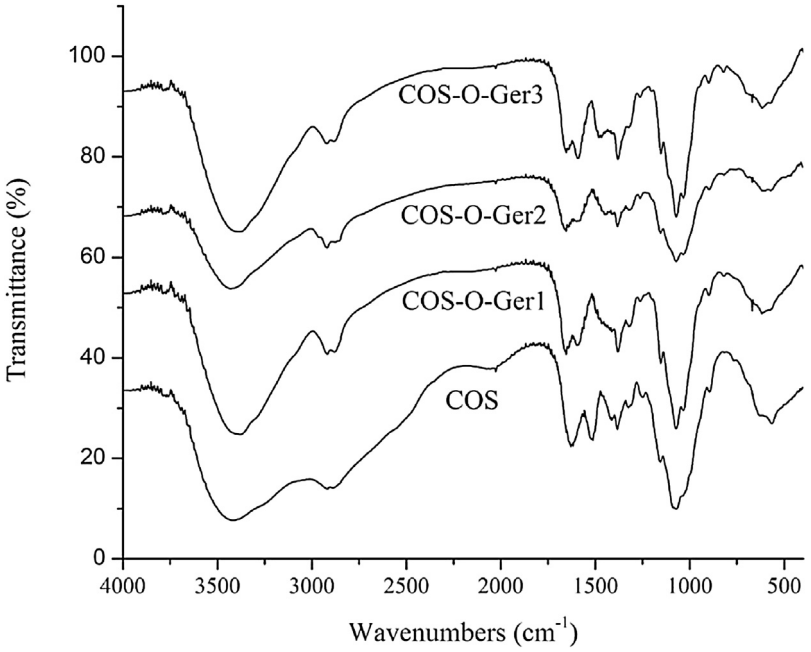

Fig. 3. FT-IR spectra of COS and COS-O-Ger1-3.

hydrogen bonding of COS molecules. At 2931 cm^{-1} was a weak band (Kamari, Aljafree, & Yusoff, 2016), which could be attributed to the C—H asymmetric/symmetric bends of the —CH_2 present in COS. The characteristic bands at 1624, 1518 and 1383 cm^{-1} were observed due to the amide one, stretching ν C—O, the amine two, bending δ N—H and amide three absorption band of COS (Zhao, Wang, Tan, Sun, & Dong, 2013), respectively. Furthermore, the asymmetric stretching of C—O—C bridge was observed at 1155 cm^{-1} (Appunni, Rajesh, & Prabhakar, 2016).The FT-IR spectra of COS-O-Ger1-3 samples were quite similar to those of COS. The absorption bands at 2920 cm^{-1} were broadened and became spiculate. The characteristic absorption band of the stretching ν C—O amide one was slightly shifted from 1624 cm^{-1} to 1655 cm^{-1} due to attachment of C=C (Zhou, Lu, Chen, & Wu, 1993). The results suggested that COS-O-Ger1-3 were successfully synthesized.

3.1.3. *^{1}H NMR spectroscopy analysis of COS-O-Ger*

^{1}H NMR spectrum of COS-O-Ger2 (A), COS (B) and Ger (C) were shown in Fig. 4. It can be found that the ^{1}H NMR spectra demonstrate all the characteristic peaks belonging to Ger, as was shown in Fig. 4C. The signals at 1.57, 1.59 and 1.65 ppm can be attributed to the proton assignment of —CH_3 of Ger (Wang, Li, Chen, Wang, & Li, 2001). Meanwhile, the triple peaks at 5.09 and 5.31 ppm were assigned to the —C=C— group of Ger (Baryshnikova, Niyazymbetov, Bogdanov, & Petrosyan, 1989), and the triple peak at 4.49 ppm was contributed by —OH proton. Furthermore, the multiplets at 3.98,

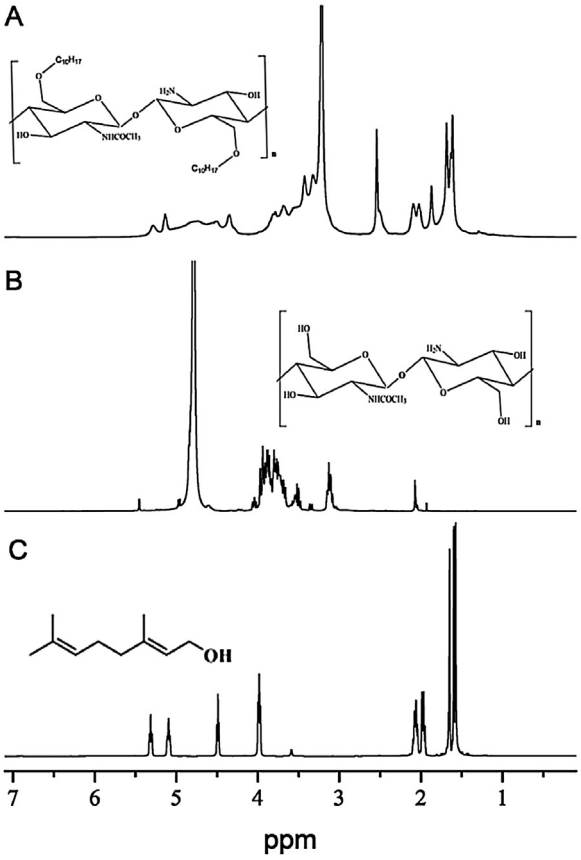

Fig. 4. ^{1}H NMR spectrum of COS-O-Ger2 (A), COS (B) and Ger (C).

2.07 and 1.98 ppm were associated with the methylene proton of Ger (Murphy & Taggart, 2001). The ^{1}H NMR spectrum of COS (Fig. 4B.) at 2.07 ppm appeared due to the presence of —CH_3 of the *N*-alkylated glucosamine residue (Koshiji et al., 2016). The multiplets from 3.08 to 3.15 ppm corresponded to *N*-acetylated Glc N (Khan, Ullah et al., 2016), and the multiplets from 3.32 to 4.09 ppm were assigned to the other methine protons of glucosamine and *N*-acetylated glucosamine respectively (Synytsya et al., 2008). Five new signals can be found in Fig. 4A compared to COS, which showed at 1.56, 1.63, 1.81, 5.08 and 5.21 ppm. The first three signals assigned to the proton assignment of —CH_3 of Ger, and the others were assigned to the —C=C— group of Ger. The results supported the claimed existence of geranyl group in the derivative.

3.1.4. TGA of COS-O-Ger

The TGA and DTG curves are an excellent method for evaluating the thermal properties of materials, and have been widely used to show the mechanism by which a material loses weight as a result of controlled heating (Khan, Islam et al., 2016). Fig. 5 showed the TGA curves and the first derivative of weight loss (DTG) thermograms of COS and COS-O-Ger1-3. The TGA curve of COS showed two weight-loss stages in the range from 30 to 550 °C (Lal, Arora, & Sharma, 2016). The first stage, ranging between 35–130 °C, corresponded to a weight loss of 10–15 wt% (related to the release of crystal water and the melting of amorphous structure of COS) (El-Sherbiny, Hefnawy, & Salih, 2016). At the second stage the range of COS was observed between 172 and 291 °C, and the temperature at the maximum decomposition rate of COS was 206 °C which referred to a complex process including dehydration of the saccharide rings, depolymerization and decomposition of the COS polymer (Appunni et al., 2016). COS-O-Ger1-3 were degraded in three well-distinguished steps, which were more obvious in DTG curves. The first step lied between 35 and 145 °C with a small weight loss of 10 wt% (associated with the loss of water). The second step (the main decomposition step presenting a weight loss of 45–50 wt%) was recorded in the temperature range of 206–349 °C. COS-O-Ger1-3 had similar curves, which showed a maximum weight loss rate occurred at about 270 °C (Rahmani et al., 2016), which indicated a better thermal stability of COS-O-Ger with respect to COS. The increase of thermal stability was due to Ger, which was successfully grafted and accordingly changed the molecular structure of COS (Srivastava & Pandey, 2002). The third step lied between 380–450 °C. It corresponded to a very small weight loss (5–8 wt%), and maybe associated with COS deacetylation (Kyzas, Siafaka, Lambropoulou, Lazaridis, & Bikiaris, 2014) or decomposition of geranyl, although futher research is necessary.

3.1.5. XRD analysis of COS-O-Ger

The structural changes in the samples were further investigated by means of the XRD patterns (Baran, Inanan, & Mentes, 2016). The XRD of COS and COS-O-Ger1-3 were depicted in Fig. 6. It can be seen that they all had one major peak, but some differences were identified in peak height, width and position between them (Anbinder, Macchi, Amalvy, & Somoza, 2016). Regarding for the characteristic of crystallinity of COS, it had two peaks at 11° and 21° respectively, as was revealed previously (Liu, 2004; Zhang et al., 2016). In contrast, the maximum peak of COS-O-Ger shifted down to 20°, and showed a relatively sharper peak, and the peak at 11° was wider and weaker. The XRD analyses suggests that as the intensity of the peaks of X-ray diffraction get sharper, crystallization is inclined to be better. This is probably due to alterative intermolecular and intra-molecular hydrogen bonding. Obviously, Ger was grafted on COS successfully, which changed the molecular structure of COS and increased its crystal domain.

3.2. Solubility of COS-O-Ger

It was well established that Ger had a poor solubility in water but was soluble in organic solvents. The solubility of COS, Ger and COS-O-Ger1-3 were investigated, and the results were summarized in Supporting Information (Supplemental Table 1). The results showed that COS did not dissolve in the acetone and diethyl ether (Khan, Ullah et al., 2016), but did dissolve in the other five solvents (distilled water, anhydrous ethanol, glacial acetic acid, DMSO and DMF). Ger had a better solubility in organic solvents compared with COS, but was insoluble in water. However, COS-O-Ger1-3 could be dissolved in all of the solvents except acetone, and readily dissolved in distilled water at neutral pH 7.0 ± 0.04. In these solvents, COS-O-Ger1-3 showed an improved solubility compared with COS and Ger. The effect of pH on water solubility of COS and COS-O-Ger1-3 was shown in Fig. 7. COS solution had a good solubility at a wide pH range (1–10) (Qin et al., 2006). At low pH (pH < 6.0), the transmittance for COS-O-Ger1-3 solutions were close to 99% as well as COS solution. The transmittance of COS-O-Ger1-3 solutions rapidly decreased and the solution became opaque as the pH was increased from 7.0 to 9.0. Ger (A) was insoluble, whereas COS (B) and COS-O-Ger2 (C) were soluble in distilled water (pH 7.0 ± 0.04). These results not only indicated that COS-O-Ger1-3 had a good solubility in acidic conditions, but also suggested that COS-O-Ger1-3 had a better solubility than that of Ger in water, implying their potential for use in food areas (Liu, Liu, Esker, & Edgar, 2016).

3.3. Antibacterial activity

The antibacterial activities of COS, Ger and COS-O-Ger against *Staphylococcus aureus*, *Escherichia coli* were evaluated in Fig. 8, respectively. The results obtained during the present study revealed that COS (b), Ger (c) and COS-O-Ger (d–f) inhibited growth

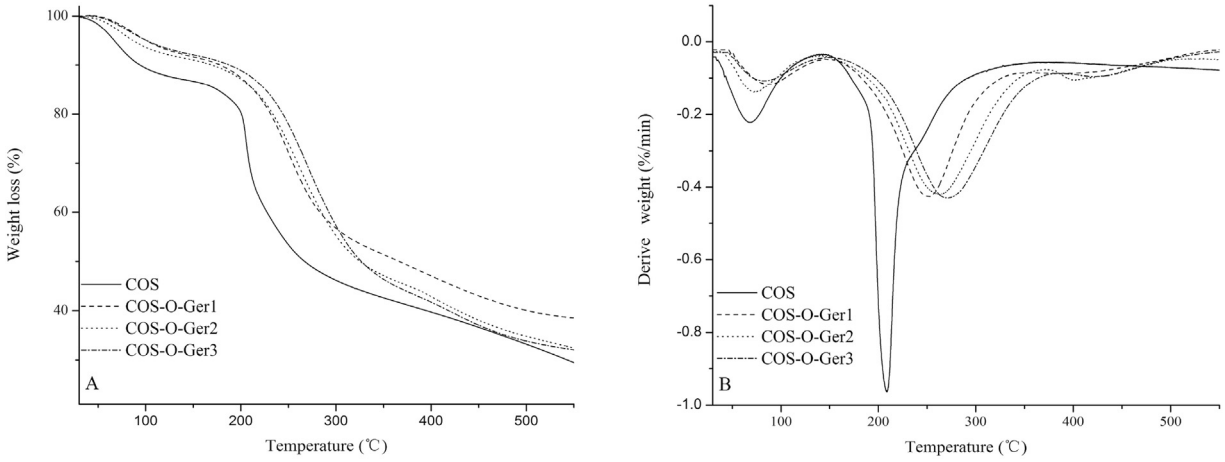

Fig. 5. Thermogravimetric curves of COS and the modified COS-O-Ger1-3.

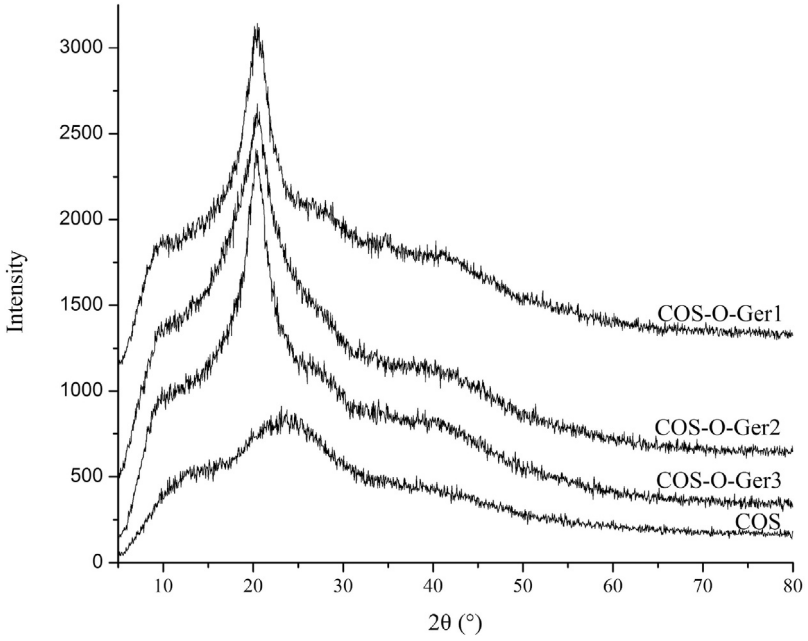

Fig. 6. XRD patterns of COS and COS-O-Ger1-3.

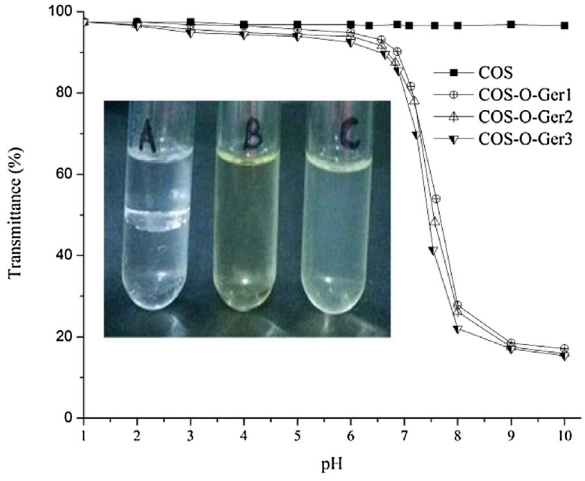

Fig. 7. pH dependence of water solubility of COS and COS-O-Ger1-3 polymer transmittance at 600 nm wavelength. Inset shows Ger (A), COS (B) and COS-O-Ger2 (C) in distilled water.

of *S. aureus* and *E. coli* as compared to control (a), confirming that the modified material had a better antibacterial activity. Fig. 8 also revealed that the antimicrobial activity of COS, Ger and COS-O-Ger against S. aureus (gram positive bacteria) was more remarkable than *E. coli* (gram negative bacteria). Similar results had also been reported by earlier reports (Aytac et al., 2016; Badawy et al., 2016; Holappa et al., 2006) and may be attributed to their different cell walls. The peptide poly-glycogen is the main components of the cell wall of *S. aureus.* The peptidoglycan layer is made up of networks with plenty of pores. Duing to the presence of these pores, COS, Ger and COS-O-Ger molecules can penetrate the cell effortlessly, leading to more rapid absorption. However, the cell wall of *E.coli* is composed of a thin membrane of peptide poly glycogen and an outer membrane constituted of lipopolysaccharide, lipoprotein, and phospholipids. Because of the complicated bilayer cell structure, the outer membrane is a potential barrier against COS, Ger and COS-O-Ger molecules (Liu, Xia et al., 2014). Moreover, it was observed that the antimicrobial activities of COS-O-Ger were enhanced with an increasing degree of substitution. These results suggested that the antimicrobial activ-

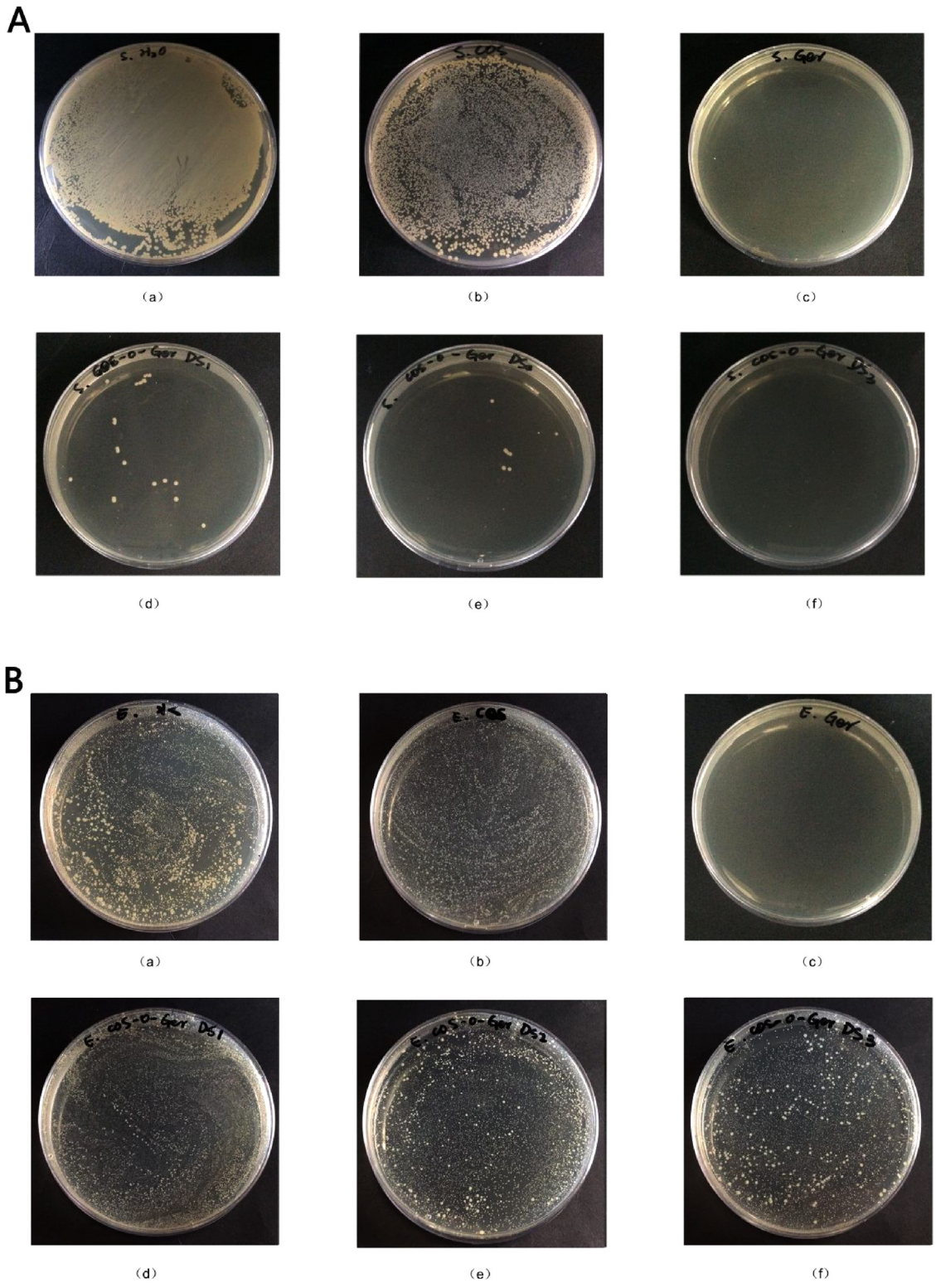

Fig. 8. Growth of *S. aureus* (A) and *E. coli* (B) in nutrient broth agar plate with (a) control, (b) COS, (c) Ger, (d) COS-O-Ger1 (DS = 0.245), (e) COS-O-Ger2 (DS = 0.342), and (f) COS-O-Ger3 (DS = 0.375).

ity of COS had been effectively improved by the introduction of Ger, and that the activity increased following the order of COS-O-Ger3 (DS = 0.375) (f) > COS-O-Ger2 (DS = 0.342) (e) > COS-O-Ger1 (DS = 0.245) (d) > COS (b). From Fig. 8 (A) and (B), it was obvious that COS-O-Ger showed a much better antibacterial activity for *S. aureus*. The result was consistent with earlier work (Khan, Ullah et al., 2016), which suggested that the antimicrobial activity of chitosan-MFA increased with the increasing degree of substitution against Gram positive and Gram negative bacteria.

4. Conclusion

In the present work, COS-O-Ger with different DS was designed and synthesized via substitution and deprotection reaction. The UV–vis, FT-IR, ^{1}H NMR and XRD analyses confirmed the structure of COS-O-Ger. TGA showed that the thermal stability of COS-O-Ger was better than that of COS, and it can be observed that the thermal stability of COS-O-Ger was enhanced with an increasing DS. COS-O-Ger exhibited a better solubility, while the solubility showed a slightly downward trend with an increasing DS. Moreover, COS-O-Ger showed a stronger antibacterial activity than COS, and the antibacterial activity increased with the increase of DS, but the inhibitory action for *S. aureus* was more remarkable than that for *E.coli*. These findings suggest that the COS-O-Ger can be used as an effective antibacterial agent. However, further study is needed to understand their mechanism of action and determine their safety. Relevant investigations are in progress.

Acknowledgements

This research was financially supported by Agricultural Science and Technology Achievement Transformation Fund (2014GB2C100312), Natural Science Foundation of Jiangsu Province (BK20160180), China Postdoctoral Science Foundation (2015M581725), Postdoctoral Science Foundation of Jiangsu province (1601200C).

Appendix A. Supplementary data

Supplementary data associated with this article can be found, in the online version, at http://dx.doi.org/10.1016/j.carbpol.2017.07.043.

References

Ahmad, M., Ahmed, S., Swami, B. L., & Ikram, S. (2015). Preparation and characterization of antibacterial thiosemicarbazide chitosan as efficient Cu(II) adsorbent. *Carbohydrate Polymers*, *132*, 164–172.

Aljawish, A., Chevalot, I., Piffaut, B., Rondeau-Mouro, C., Girardin, M., Jasniewski, J., et al. (2012). Functionalization of chitosan by laccase-catalyzed oxidation of ferulic acid and ethyl ferulate under heterogeneous reaction conditions. *Carbohydrate Polymers*, *87*(1), 537–544.

Anbinder, P., Macchi, C., Amalvy, J., & Somoza, A. (2016). Chitosan-graft-poly (n-butyl acrylate) copolymer: Synthesis and characterization of a natural/synthetic hybrid material. *Carbohydrate Polymers*, *145*, 86–94.

Appunni, S., Rajesh, M. P., & Prabhakar, S. (2016). Nitrate decontamination through functionalized chitosan in brackish water. *Carbohydrate Polymers*, *147*, 525–532.

Aytac, Z., Yildiz, Z. I., Kayaci-Senirmak, F., San Keskin, N. O., Tekinay, T., & Uyar, T. (2016). Electrospinning of polymer-free cyclodextrin/geraniol–inclusion complex nanofibers: Enhanced shelf-life of geraniol with antibacterial and antioxidant properties. *RSC Advances*, *6*(52), 46089–46099.

Badawy, M. E., Rabea, E. I., Taktak, N. E., & El-Nouby, M. A. (2016). The antibacterial activity of chitosan products blended with monoterpenes and their biofilms against plant pathogenic bacteria. *Scientifica (Cairo)*, *2016*, 1796256.

Bakkali, F., Averbeck, S., Averbeck, D., & Idaomar, M. (2008). Biological effects of essential oils–A review. *Food Chem Toxicol*, *46*(2), 446–475.

Baran, T., Inanan, T., & Mentes, A. (2016). Synthesis, characterization, and catalytic activity in Suzuki coupling and catalase-like reactions of new chitosan supported Pd catalyst. *Carbohydrate Polymers*, *145*, 20–29.

Baryshnikova, T. K., Niyazymbetov, M. E., Bogdanov, V. S., & Petrosyan, V. A. (1989). Synthesis based on electrogenerated carbenes. *Organic Chemistry*, *10*, 2327–2331.

Burt, S. (2004). Essential oils: Their antibacterial properties and potential applications in foods–A review. *International Journal of Food Microbiology*, *94*(3), 223–253.

Cassani, L., Tomadoni, B., Viacava, G., Ponce, A., & Moreira, M. R. (2016). Enhancing quality attributes of fiber-enriched strawberry juice by application of vanillin or geraniol. *LWT – Food Science and Technology*, *72*, 90–98.

Chen, W., & Viljoen, A. M. (2010). Geraniol — A review of a commercially important fragrance material. *South African Journal of Botany*, *76*(4), 643–651.

Choi, B., Kim, C., Choi, B., Yoo, Y., Kim, C., & Jung, S. (2001). In vitro antimicrobial activity of a chitooligosaccharide mixture against Actinobacillus actinomycetemcomitans and Streptococcus mutans. *International Journal of Antimicrobial Agents*, *18*, 553–557.

Dos Santos, Z. M., Caroni, A. L., Pereira, M. R., da Silva, D. R., & Fonseca, J. L. (2009). Determination of deacetylation degree of chitosan: A comparison between conductometric titration and CHN elemental analysis. *Carbohydrate Research*, *344*(18), 2591–2595.

El-Sherbiny, I. M., Hefnawy, A., & Salih, E. (2016). New core-shell hyperbranched chitosan-based nanoparticles as optical sensor for ammonia detection. *International Journal of Biological Macromolecules*, *86*, 782–788.

Feng, Y., & Xia, W. (2011). Preparation, characterization and antibacterial activity of water-soluble O-fumaryl-chitosan. *Carbohydrate Polymers*, *83*(3), 1169–1173.

Guo, Z., Xing, R., Liu, S., Zhong, Z., Ji, X., Wang, L., et al. (2007). Antifungal properties of Schiff bases of chitosan, N-substituted chitosan and quaternized chitosan. *Carbohydrate Research*, *342*(10), 1329–1332.

Holappa, J., Hjálmarsdóttir, M., Másson, M., Rúnarsson, Asplund, T., Soininen, P., et al. (2006). Antimicrobial activity of chitosan N-betainates. *Carbohydrate Polymers*, *65*(1), 114–118.

Huang, R., Mendis, E., Rajapakse, N., & Kim, S. K. (2006). Strong electronic charge as an important factor for anticancer activity of chitooligosaccharides (COS). *Life Sciences*, *78*(20), 2399–2408.

Jayakumar, R., Chennazhi, K. P., Muzzarelli, R. A. A., Tamura, H., Nair, S. V., & Selvamurugan, N. (2010). Chitosan conjugated DNA nanoparticles in gene therapy. *Carbohydrate Polymers*, *79*(1), 1–8.

Jeon, Y., & Kim, S. (2000). Production of chitooligosaccharides using an ultrafiltration membrane reactor and their antibacterial activity. *Carbohydrate Polymers*, *41*, 133–141.

Kalemba, D., & Kunicka, A. (2003). Antibacterial and antifungal properties of essential oils. *Current Medicinal Chemistry*, *10*, 813–829.

Kamari, A., Aljafree, N. F., & Yusoff, S. N. (2016). N,N-Dimethylhexadecyl carboxymethyl chitosan as a potential carrier agent for rotenone. *International Journal of Biological Macromolecules*, *88*, 263–272.

Khan, Y. H., Islam, A., Sarwar, A., Gull, N., Khan, S. M., Munawar, M. A., et al. (2016). Novel green nano composites films fabricated by indigenously synthesized graphene oxide and chitosan. *Carbohydrate Polymers*, *146*, 131–138.

Khan, I., Ullah, S., & Oh, D. H. (2016). Chitosan grafted monomethyl fumaric acid as a potential food preservative. *Carbohydrate Polymers*, *152*, 87–96.

Kim, S., & Rajapakse, N. (2005). Enzymatic production and biological activities of chitosan oligosaccharides (COS): A review. *Carbohydrate Polymers*, *62*(4), 357–368.

Koshiji, K., Nonaka, Y., Iwamura, M., Dai, F., Matsuoka, R., & Hasegawa, T. (2016). C6-Modifications on chitosan to develop chitosan-based glycopolymers and their lectin-affinities with sigmoidal binding profiles. *Carbohydrate Polymers*, *137*, 277–286.

Kyzas, G. Z., Siafaka, P. I., Lambropoulou, D. A., Lazaridis, N. K., & Bikiaris, D. N. (2014). Poly(itaconic acid)-grafted chitosan adsorbents with different cross-linking for Pb(II) and Cd(II) uptake. *Langmuir*, *30*(1), 120–131.

Lal, S., Arora, S., & Sharma, C. (2016). Synthesis, thermal and antimicrobial studies of some Schiff bases of chitosan. *Journal of Thermal Analysis and Calorimetry*, *124*(2), 909–916.

Liu, J., Lu, J. F., Kan, J., Tang, Y. Q., & Jin, C. H. (2013). Preparation: Characterization and antioxidant activity of phenolic acids grafted carboxymethyl chitosan. *International Journal of Biological Macromolecules*, *62*, 85–93.

Liu, H. (2004). Structural characterization and antimicrobial activity of chitosan/betaine derivative complex. *Carbohydrate Polymers*, *55*(3), 291–297.

Liu, S., Liu, J., Esker, A. R., & Edgar, K. J. (2016). An efficient, regioselective pathway to cationic and zwitterionic N-Heterocyclic cellulose ionomers. *Biomacromolecules*, *17*(2), 503–513.

Liu, H., Liu, X., Yue, L., Jiang, Q., & Xia, W. (2016). Synthesis, characterization and bioactivities of N,O-carbonylated chitosan. *International Journal of Biological Macromolecules*, *91*, 220–226.

Liu, X., Xia, W., Jiang, Q., Xu, Y., & Yu, P. (2014). Synthesis, characterization, and antimicrobial activity of kojic acid grafted chitosan oligosaccharide. *Journal of Agricultural and Food Chemistry*, *62*(1), 297–303.

Liu, K., Xu, Y., Lin, X., Chen, L., Huang, L., Cao, S., et al. (2014). Synergistic effects of guanidine-grafted CMC on enhancing antimicrobial activity and dry strength of paper. *Carbohydrate Polymers*, *110*, 382–387.

Másson, M., Holappa, J., Hjálmarsdóttir, M., Rúnarsson, V., Nevalainen, T., & Järvinen, T. (2008). Antimicrobial activity of piperazine derivatives of chitosan. *Carbohydrate Polymers*, *74*(3), 566–571.

Ma, G., Yang, D., Kennedy, J. F., & Nie, J. (2009). Synthesize and characterization of organic-soluble acylated chitosan. *Carbohydrate Polymers*, *75*(3), 390–394.

Moreno-Vasquez, M. J., Valenzuela-Buitimea, E. L., Plascencia-Jatomea, M., Encinas-Encinas, J. C., Rodriguez-Felix, F., Sanchez-Valdes, S., et al. (2017). Functionalization of chitosan by a free radical reaction: Characterization, antioxidant and antibacterial potential. *Carbohydrate Polymers*, *155*, 117–127.

Murphy, A., & Taggart, G. (2001). Synthesis and characterisation of a novel surfactant: Sodiumgeranyl sulphate. *Colloids and Surfaces A: Physicochemical and Engineering Aspects*, *180*, 295–299.

Qin, C., Li, H., Xiao, Q., Liu, Y., Zhu, J., & Du, Y. (2006). Water-solubility of chitosan and its antimicrobial activity. *Carbohydrate Polymers*, *63*(3), 367–374.

Rahman, M. H., Hjeljord, L. G., Aam, B. B., Sørlie, M., & Tronsmo, A. (2014). Antifungal effect of chito-oligosaccharides with different degrees of polymerization. *European Journal of Plant Pathology*, *141*(1), 147–158.

Rahmani, S., Mohammadi, Z., Amini, M., Isaei, E., Taheritarigh, S., Rafiee Tehrani, N., et al. (2016). Methylated 4-N, N dimethyl aminobenzyl N, O carboxymethyl chitosan as a new chitosan derivative: Synthesis, characterization, cytotoxicity and antibacterial activity. *Carbohydrate Polymers*, *149*, 131–139.

Shen, K. T., Chen, M. H., Chan, H. Y., Jeng, J. H., & Wang, Y. J. (2009). Inhibitory effects of chitooligosaccharides on tumor growth and metastasis. *Food and Chemical Toxicology*, *47*(8), 1864–1871.
Solorzano-Santos, F., & Miranda-Novales, M. G. (2012). Essential oils from aromatic herbs as antimicrobial agents. *Current Opinion in Biotechnology*, *23*(2), 136–141.
Srivastava, A. K., & Pandey, P. (2002). Synthesis and characterisation of copolymers containing geraniol and styrene initiated by benzoyl peroxide. *European Polymer Journal*, *38*, 1709–1712.
Sun, T., Yao, Q., Zhou, D., & Mao, F. (2008). Antioxidant activity of N-carboxymethyl chitosan oligosaccharides. *Bioorganic & Medicinal Chemistry*, *18*(21), 5774–5776.
Synytsya, A., Blafková, P., Synytsya, A., Čopíková, J., Spěváček, J., & Uher, M. (2008). Conjugation of kojic acid with chitosan. *Carbohydrate Polymers*, *72*(1), 21–31.
Tomadoni, B., Cassani, L., Moreira, M. R., & Ponce, A. (2015). Efficacy of vanillin and geraniol in reducing Escherichia coli O157:H7 on strawberry juice. *LWT – Food Science and Technology*, *64*(2), 554–557.
Vela Gurovic, M. S., Dello Staffolo, M., Montero, M., Debbaudt, A., Albertengo, L., & Rodriguez, M. S. (2015). Chitooligosaccharides as novel ingredients of fermented foods. *Food & Function*, *6*(11), 3437–3443.
Wang, J., & Wang, H. (2011). Preparation of soluble p-aminobenzoyl chitosan ester by Schiff's base and antibacterial activity of the derivatives. *International Journal of Biological Macromolecules*, *48*(3), 523–529.
Wang, Y., Li, L., Chen, J., Wang, Q., & Li, Y. (2001). First total synthesis of 7-O-geranyl-pseudobaptigenin. *Chinese Chemical Letters*, *12*, 409–410.
Wang, Z., Zheng, L., Li, C., Zhang, D., Xiao, Y., Guan, G., et al. (2015). Modification of chitosan with monomethyl fumaric acid in an ionic liquid solution. *Carbohydrate Polymers*, *117*, 973–979.
Xia, W., Liu, P., Zhang, J., & Chen, J. (2011). Biological activities of chitosan and chitooligosaccharides. *Food Hydrocolloids*, *25*(2), 170–179.
Yan, F., Dang, Q., Liu, C., Yan, J., Wang, T., Fan, B., et al. (2016). 3,6-O-[N-(2-Aminoethyl)-acetamide-yl]-chitosan exerts antibacterial activity by a membrane damage mechanism. *Carbohydrate Polymers*, *149*, 102–111.
Yegin, Y., Perez-Lewis, K. L., Zhang, M., Akbulut, M., & Taylor, T. M. (2016). Development and characterization of geraniol-loaded polymeric nanoparticles with antimicrobial activity against foodborne bacterial pathogens. *Journal of Food Engineering*, *170*, 64–71.
Zhang, X., Wang, H., Wen, X., Zhang, A., Wang, X., Zhong, L., et al. (2016). Synthesis and characterization of xylan grafted with polyethylene glycol in ionic liquid and their use as moisture-absorption/retention biomaterials. *Macromolecular Materials and Engineering*, *301*(3), 287–295.
Zhao, D., Wang, J., Tan, L., Sun, C., & Dong, J. (2013). Synthesis of N-furoyl chitosan and chito-oligosaccharides and evaluation of their antioxidant activity in vitro. *International Journal of Biological Macromolecules*, *59*, 391–395.
Zhou, J., Lu, G., Chen, Z., & Wu, S. (1993). Reqioselective synthesis of linalyl compounds via addition reaction of qeranyl bromide and tin with carbonyl compounds. *Chinese Journal of Chemistry*, *11*, 164–168.
Zou, P., Yang, X., Wang, J., Li, Y., Yu, H., Zhang, Y., et al. (2016). Advances in characterisation and biological activities of chitosan and chitosan oligosaccharides. *Food Chemistry*, *190*, 1174–1181.